BJP BRITISH JOURNAL OF PHARMACOLOGY

BPS BRITISH PHARMACOLOGICAL SOCIETY

British Journal of Pharmacology (2010), 159, 1532–1541

0007-1188/10
www.brjpharmacol.org

RESEARCH PAPER

The anti-protozoal drug pentamidine blocks $K_{IR}2.x$-mediated inward rectifier current by entering the cytoplasmic pore region of the channel

TP de Boer[1], L Nalos[1], A Stary[2], B Kok[1], MJC Houtman[1], G Antoons[1], TAB van Veen[1], JDM Beekman[1], BL de Groot[2], T Opthof[1], MB Rook[1], MA Vos[1] and MAG van der Heyden[1]

[1]*Department of Medical Physiology, Division Heart & Lungs, UMCU, Utrecht, The Netherlands; and* [2]*The Computational Biomolecular Dynamics Group, Max Planck Institute for Biophysical Chemistry, Göttingen, Germany*

Background and purpose: Pentamidine is a drug used in treatment of protozoal infections. Pentamidine treatment may cause sudden cardiac death by provoking cardiac arrhythmias associated with QTc prolongation and U-wave alterations. This proarrhythmic effect was linked to inhibition of hERG trafficking, but not to acute block of ion channels contributing to the action potential. Because the U-wave has been linked to the cardiac inward rectifier current (I_{K1}), we examined the action and mechanism of pentamidine-mediated I_{K1} block.
Experimental approach: Patch clamp measurements of I_{K1} were made on cultured adult canine ventricular cardiomyocytes, $K_{IR}2.1$-HEK293 cells and $K_{IR}2.x$ inside-out patches. Pentamidine binding to cytoplasmic amino acid residues of $K_{IR}2.1$ channels was studied by molecular modelling.
Key results: Pentamidine application (24 h) decreased I_{K1} in cultured canine cardiomyocytes and $K_{IR}2.1$-HEK293 cells under whole cell clamp conditions. Pentamidine inhibited I_{K1} in $K_{IR}2.1$-HEK293 cells 10 min after application. When applied to the cytoplasmic side under inside-out patch clamp conditions, pentamidine block of I_{K1} was acute (IC_{50} = 0.17 μM). Molecular modelling predicted pentamidine-channel interactions in the cytoplasmic pore region of $K_{IR}2.1$ at amino acids E224, D259 and E299. Mutation of these conserved residues to alanine reduced pentamidine block of I_{K1}. Block was independent of the presence of spermine. $K_{IR}2.2$, and $K_{IR}2.3$ based I_{K1} was also sensitive to pentamidine blockade.
Conclusions and implications: Pentamidine inhibits cardiac I_{K1} by interacting with three negatively charged amino acids in the cytoplasmic pore region. Our findings may provide new insights for development of specific I_{K1} blocking compounds.
British Journal of Pharmacology (2010) **159,** 1532–1541; doi:10.1111/j.1476-5381.2010.00658.x; published online 24 February 2010

Keywords: inward rectifier current; I_{K1}; $K_{IR}2.1$; pentamidine; ECG; arrhythmia; molecular modelling

Abbreviations: AP, action potential; ATS1, Andersen-Tawil syndrome; HEK-KWGF, human embryonic kidney cell line stably expressing GFP-tagged inward rectifier channel protein $K_{IR}2.1$; hERG, human ether-a-go-go related gene; I_{K1}, inward rectifier current; I_{Kr}, delayed rectifier current; $K_{IR}2.x$, inward rectifier channel subunit; QT(c), Q-T time interval on electrocardiogram corrected for heart rate

Introduction

The ventricular cardiac action potential (AP) has a long plateau and repolarization phase, essential for contractility and recovery of excitability. Between successive APs, there is a constant resting membrane potential based on potent inward rectifier current (I_{K1}). In mammals, the *KCNJ2* and *KCNJ12* gene products $K_{IR}2.1$ and $K_{IR}2.2$ (nomenclature follows Alexander *et al.*, 2009) constitute the main determinants of I_{K1} in the ventricle (Dhamoon and Jalife, 2005). In addition, $K_{IR}2.3$ encoded by the *KCNJ4* gene contributes to cardiac I_{K1}. Inhibition of endogenous I_{K1} by dominant negative $K_{IR}2.1$ expression in the working ventricular myocardium of guinea pigs induces ectopic pacemaker activity (Miake *et al.*, 2002). In humans, loss-of-function mutations in $K_{IR}2.1$ correlates with Andersen-Tawil syndrome (ATS1) characterized by ventricular arrhythmias, periodic paralysis and dysmorphic features (Plaster *et al.*, 2001; Tristani-Firouzi *et al.*, 2002). ATS1 is associated with the appearance of more prominent U waves (Zhang *et al.*, 2005a; Nagase *et al.*, 2007).

Correspondence: Marcel AG van der Heyden, Department of Medical Physiology, Division Heart and Lungs, University Medical Center Utrecht, Yalelaan 50, 3584 CM Utrecht, The Netherlands. E-mail: m.a.g.vanderheyden@umcutrecht.nl
Received 20 August 2009; revised 23 October 2009; accepted 25 November 2009

Acquired ion channel dysfunction, either by loss or gain of function, may result in a wide variety of cardiac arrhythmias (Kannankeril and Roden, 2007; Murphy and Dargie, 2007). The ion current involved is often the $K_v11.1$ (human ether-a-go-go related gene; hERG)-based, rapid component of the delayed rectifier current (I_{Kr}). Unfortunately, non-cardiac drugs may affect this current, but many other currents as well. Recently, the widely used antimalarial drug chloroquine and the oestrogen receptor antagonist tamoxifen were demonstrated to inhibit $K_{IR}2.1$-based I_{K1} by blocking the ion channel pore from the cytoplasmic side or by interfering in the $K_{IR}2.1$–PIP_2 interaction, respectively (Rodríguez-Menchaca *et al.*, 2008; Ponce-Balbuena *et al.*, 2009).

Pentamidine belongs to the diamine family used for treatment of pathogenic protozoal infections causing human African trypanosomis (sleeping sickness), visceral Leishmaniasis (Bray *et al.*, 2003), and opportunistic pathogenic infections causing candidiasis and pneumonia in immunocompromised individuals, such as HIV-positive patients (Sands *et al.*, 1985; Goa and Campoli-Richards, 1987). Clinically, pentamidine has been associated with QTc prolongation, U-wave amplitude increase, U-wave alternans and Torsades de Pointes arrhythmias with and without electrolyte abnormalities (Bibler *et al.*, 1988; Mitchell *et al.*, 1989; Gonzalez *et al.*, 1991; Quadrel *et al.*, 1992; Eisenhauer *et al.*, 1994; Girgis *et al.*, 1997). Recently, pentamidine has been shown to reduce I_{Kr} and to prolong the AP, because it hampers transport of the $K_v11.1$ ion channel protein towards the sarcolemma (Cordes *et al.*, 2005; Kuryshev *et al.*, 2005). Although this might explain QTc prolongation, U-wave alterations remain unexplained. Given the similarity between alterations in U-wave morphology under conditions of *KCNJ2* mutations and pentamidine administration, we have assessed whether pentamidine affects the inward rectifier current and its mode of action at the molecular level.

We demonstrate that (i) pentamidine inhibits I_{K1} in isolated adult ventricular cardiac myocytes at clinical concentrations; that (ii) it produces acute block of $K_{IR}2.x$ (inward rectifier channel subunit)-based I_{K1} by plugging the pore region from the cytoplasmic side; that (iii) the acidic amino acid residues E224, D259 and E299 of $K_{IR}2.1$ are directly involved in pentamidine-mediated block of the outward I_{K1}.

Methods

Cell culture

All animal care and experimental procedures conformed to the Guide for the Care and Use of Laboratory Animals published by the US National Institutes of Health (NIH Publication no. 85-23, revised 1996) and was approved by the institutional committee for animal experiments. Left ventricular myocytes from adult dogs were isolated and GFP-tagged $K_{IR}2.1$ HEK293 (human embryonic kidney cell line stably expressing GFP-tagged inward rectifier channel protein $K_{IR}2.1$; HEK-KWGF) cells were generated and cultured as described previously (De Boer *et al.*, 2006a,b). In inside-out experiments, HEK293T cells were transfected with 20 ng KCNJx cDNA and 6 ng EGFP per cm^2 and used within 48 h. Mouse KCNJ2, KCNJ12 and KCNJ4 pCXN2 expression constructs and human wild type E224A, F254A, D259A and E299A mutant KCNJ2 constructs have been described previously (Ishihara and Ehara, 2004; Rodríguez-Menchaca *et al.*, 2008).

Pentamidine

Pentamidine-isethionate (Pentacarinat® 300, Sanofi Aventis, Gouda, The Netherlands) was dissolved in water to provide a stock solution of 0.1 M, sterilized by filtration (0.22 µm), aliquoted and stored at –20°C until use.

Western blotting

Cells were lysed in RIPA buffer [20 mM Tris-HCl, pH 7.4, 150 mM NaCl, 10 mM Na_2HPO_4, 1% (v/v) Triton X-100, 1% (w/v) Na-deoxycholate, 0.1% (w/v) SDS, 1 mM EDTA, 50 mM NaF, 2 mM PMSF and 14 $\mu g \cdot mL^{-1}$ aprotinin]. Lysates were clarified by centrifugation at 14 000× *g* for 10′ at 4°C and mixed with loading buffer. Twenty-five micrograms of proteins were separated by 10% SDS-PAGE and blotted onto nitrocellulose membrane (Bio-Rad, Veenendaal, Netherlands). Protein transfer was assessed by Ponceau S staining (Sigma, St Louis, MO, USA). After blocking with 5% non-fat milk, blots were incubated with $K_{IR}2.1$ (Cat. no. sc-28633; Santa Cruz Biotechnology, Santa Cruz, CA, USA) and Cadherin (Cat. no. C1821; Sigma) antibodies for adult cardiomyocytes, or GFP antibody (Cat. no. sc-9996; Santa Cruz Biotechnology) for HEK-KWGF cells. Finally, peroxidase-conjugated secondary antibody (Jackson ImmunoResearch, West Grove, PA, USA) was applied. Standard ECL procedure was used as final detection (Amersham Bioscience, Buckinghamshire, UK). ImageQuant TL software (Amersham) was used for signal quantification.

Electrophysiology

Patch clamp measurements were made using a HEKA EPC-10 Double Plus amplifier controlled by PatchMaster 2.10 software (HEKA, Lambrecht/Pfalz, Germany). Voltage clamp measurements of whole cell I_{K1} were made by applying 1 s test pulses ranging between –120 and +40 mV, with 10 mV increments, from a holding potential of –40 mV and with minimal series resistance compensation of 70%. Steady-state current at the end of the pulse was normalized to cell capacitance and plotted versus test potential. Inside-out patch-clamp measurements of I_{K1} were made in absence of Mg^{2+} as described previously (Ishihara and Ehara, 2004). Excised membrane patches were placed close to the inflow region of the recording chamber, and experiments were started after inward rectification due to endogenous polyamines had disappeared as completely as possible. Currents were elicited using a ramp protocol, from –100 to 100 mV in 5 s, starting at a holding potential of –40 mV. Recorded current traces were normalized to the holding current at –40 mV obtained from the control traces. After recording control traces, excised membrane patches were exposed to bath solution containing spermine and/or pentamidine. For determination of IC_{50}, each excised membrane patch was exposed to a series of pentamidine concentrations. Fractional block of outward I_{K1} was calculated

using current level at +50 mV, and values obtained with experimental solutions were divided by corresponding values from the previously recorded control trace. Patch pipettes were made with a Sutter P-2000 puller (Sutter Instrument, Novato, CA, USA), and had resistances of 2–3 MΩ. Extracellular solution for whole cell I_{K1} measurements contained (in mmol·L^{-1}): NaCl 140, KCl 5.4, $CaCl_2$ 1, $MgCl_2$ 1, glucose 6, $NaHCO_3$ 17.5, HEPES 15, pH 7.4/NaOH. The pipette solution contained potassium gluconate 125, KCl 10, HEPES 5, EGTA 5, $MgCl_2$ 2, $CaCl_2$ 0.6, Na_2ATP 4, pH 7.20/KOH. Inside-out experiments were done with a bath solution containing: KCl 125, EDTA (2K) 4, K_2HPO_4 7.2, KH_2PO_4 2.8, pH 7.20/KOH. The pipette solution contained KCl 145, $CaCl_2$ 1, HEPES 5, pH 7.40/KOH.

Molecular modeling and ligand docking

Pentamidine was docked into the crystal structure of the cytoplasmic $K_{IR}2.1$ domain (pdb identifier: 1U4F) (Pegan *et al.*, 2005). Drug coordinates were obtained from the ZINC database (Irwin and Shoichet, 2005). FlexX (version 1.20.1) in Sybyl8.0 (Tripos International, St. Louis, MI, USA) was used to randomly dock pentamidine (n = 100) into the cytoplasmic cavity of $K_{IR}2.1$ using default parameters. Ligand partial charges were calculated with the Gasteiger–Hückel method. Modelling was visualized with Pymol software (Delano Scientific, Palo Alto, CA, USA). Modelling, docking and visualization were performed on a Linux 4 Intel Core2 Quad workstation, SUSE Linux 10.2 operating system (Novell Inc., Waltham, MA, USA).

Statistics

Group averages are presented as mean ± standard error of mean, and were tested for significance using Student's *t*-test (two groups) or an ANOVA test with a Holm's *post hoc* test when more than two groups were involved. Analysis was done using Kaleidagraph 4.0 (Synergy Software, Reading, PA, USA), with the significance level at $P < 0.05$.

Results

Pentamidine inhibits cardiac I_{K1}

Based on the findings of pentamidine-associated U-wave alterations in patients and a correlation between the U-wave and I_{K1}, we hypothesized that pentamidine might inhibit I_{K1} in cardiac myocytes. Figure 1 and Table 1 show that pentamidine treatment at 10 μM for a period of 24 h inhibited the inward and outward components of I_{K1} by 62 and 73%, respectively, in adult canine ventricular myocytes (Figure 1A and C, Table 1). One micromolar pentamidine appeared to yield mild inhibition, but this inhibitory effect did not reach significance, even when the period of application was prolonged from 24 to 48 h. Furthermore, pentamidine substantially changed the kinetics of the inward component; the time to 90% of maximal activity increased almost 30-fold (Table 1). $K_{IR}2.1$ protein expression levels as assessed by Western blot revealed no decrease at 24 h and 18% decrease at 48 h of 10 μM pentamidine incubation (Figure 1D).

Cardiac I_{K1} is mainly determined by $K_{IR}2.1$ protein. Therefore, we analyzed whether $K_{IR}2.1$ based I_{K1} density is sensitive to pentamidine in HEK293 cells stably expressing GFP-tagged $K_{IR}2.1$ (HEK-KWGF). Under these conditions, the effects of pentamidine were even stronger. Even 1 μM pentamidine applied for 24 h reduced the inward (66%) and outward component of I_{K1} (94%) with virtually complete blockade at 10 μM pentamidine (Figure 1B and C, Table 1). At the protein level, a 17, 35 and 50% inhibition of expression levels was found at 16, 24 and 48 h of incubation with 10 μM pentamidine, respectively.

Pentamidine acutely blocks I_{K1} channels when applied from the cytoplasmic side

To further explore the time relationship between pentamidine application and I_{K1} block, the drug was infused during continuous I_{K1} measurement. Figure 2A shows that acute application of 10 μM pentamidine decreased I_{K1} after 10 min in HEK-KWGF cells in the whole cell patch mode. Altered opening kinetics of the inward component was seen from that time onwards (inset). This effect was slow, because pentamidine acts from the cytoplasmic side of the ion channel as can be appreciated from the data in the inside-out patch configuration (Figure 2A), resulting in an IC_{50} of 0.17 ± 0.04 μM and a Hill coefficient of –0.87 ± 0.10 (n = 11) (Figure 2B and C).

We next compared pentamidine-mediated block with that of chloroquine, which is known to inhibit the I_{K1} ion channel acutely with an IC_{50} of 1.1 ± 0.2 μM (Rodríguez-Menchaca *et al.*, 2008). Figure 2D shows the block of I_{K1} by 1 μM pentamidine and by 1 μM chloroquine. Chloroquine outward current block was 70%, pentamidine caused a 95% block. Although inward current was less affected by both drugs, pentamidine was again more potent than chloroquine. No additive effects were seen when applying the two drugs together (not shown).

Direct pentamidine block depends on negatively charged residues in the $K_{IR}2.1$ cytoplasmic pore region.

As the direct effects of pentamidine on $K_{IR}2.1$-based I_{K1} reflect those observed for chloroquine (Rodríguez-Menchaca *et al.*, 2008), we next assessed whether pentamidine is also able to enter the cytoplasmic pore region and with which amino acids it interacts. Molecular modelling was used to examine potential physical interaction sites of the $K_{IR}2.1$ channel with pentamidine (structure shown at top of Figure 3). Figure 3B and C show the preferential orientation of pentamidine within the cytoplasmic cavity. Pentamidine adopts a U-shaped binding conformation, and favourable interactions with residues E224, D259 and E299 are predicted. The carboxylate oxygen atoms of E224 from two opposing subunits form hydrogen bonds with the protons of the amino moiety of the benzamidine rings from pentamidine. Hydrogen bonds are also formed between the backbone oxygen of E299 and two nitrogen atoms of pentamidine. Furthermore, the carboxylate oxygen of D259 from subunit B interacts favourably with the amino group of one of the benzamidine rings.

Using inside-out patches, Figure 4A ('wild type') and B ('$K_{IR}2.1$') show that wild-type human $K_{IR}2.1$ I_{K1} channels are very effectively blocked (95%) by 1 μM pentamidine.

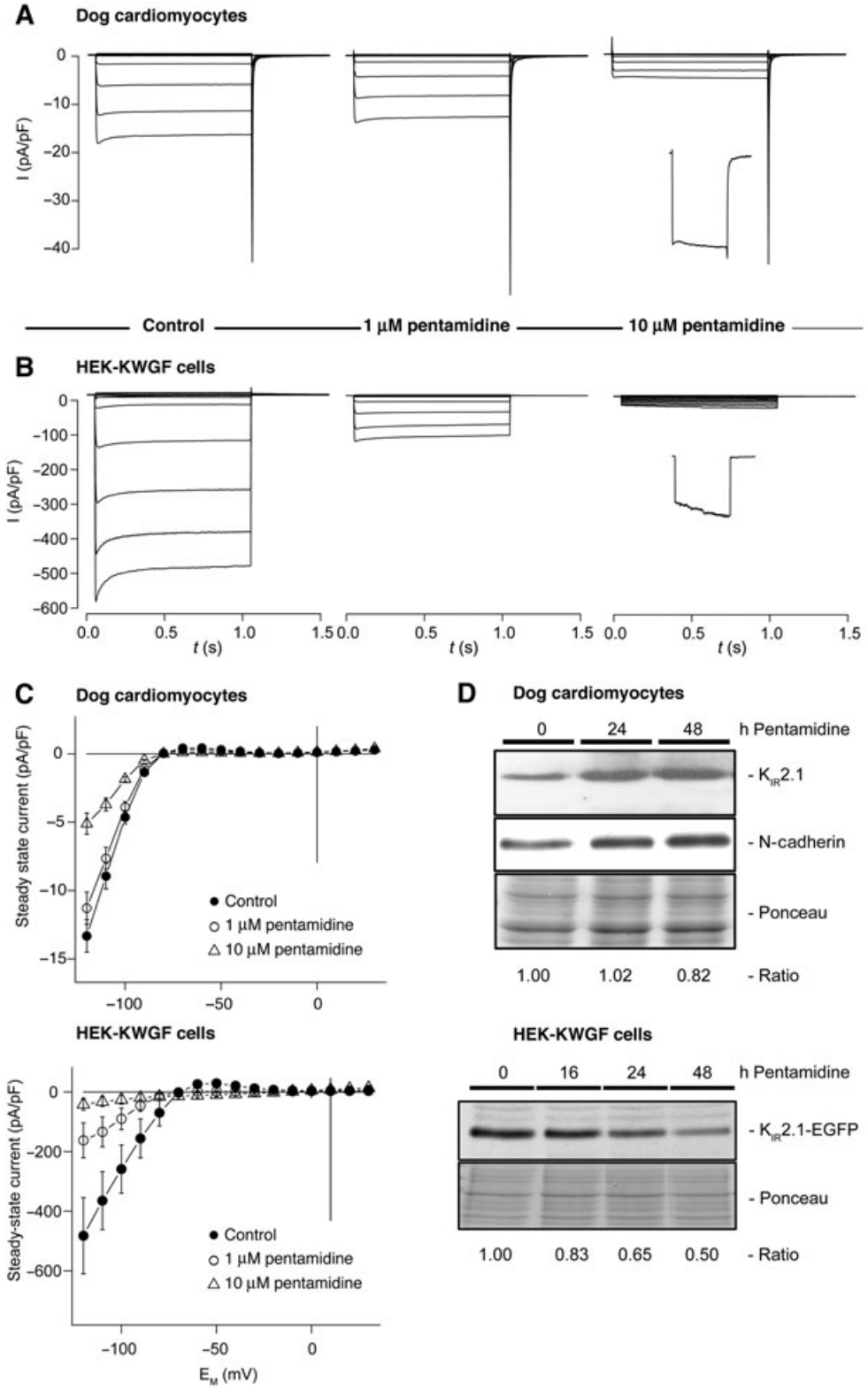

Figure 1 Pentamidine inhibits I_{K1} in cultured cardiomyocytes. Treatment for 24 h with pentamidine decreased I_{K1} densities in cultured adult dog cardiomyocytes (A, C) and HEK-KWGF cells (B, C). Besides reduced current levels, also inward current activation was slowed, as can be seen with 10 μM pentamidine in dog cardiomyocytes, and more pronounced with HEK-KWGF cells (see insets depicting currents evoked by a step to –120 mV) (A, B). Representative image ($n = 2$) of $K_{IR}2.1$ expression in cultured adult cardiomyocytes in time (h) following pentamidine treatment (10 μM) as determined by Western blot, N-cadherin and Ponceau staining serve as loading control for quantification (D, upper panel). Representative image ($n = 3$) of $K_{IR}2.1$-GFP expression in HEK-KWGF cells after pentamidine treatment (10 μM) as determined by Western blot, Ponceau staining serves as loading control for quantification (D, lower panel). HEK-KWGF, human embryonic kidney cell line stably expressing GFP-tagged inward rectifier channel protein $K_{IR}2.1$.

Table 1 Twenty-four-hour pentamidine treatment alters I_{K1} characteristics

	Adult dog cardiomyocytes		*HEK-KWGF*		
	Control	*10 μM*	*Control*	*1 μM*	*10 μM*
Max. outward current (pA/pF)	0.30 ± 0.04 (6)	0.08 ± 0.02 (6)	29.0 ± 8.0 (6)	1.6 ± 1.1 (9)	–9.4 ± 7.2 (6)
Max. inward current (pA/pF)	–13.3 ± 1.2 (6)	–5.1 ± 0.1 (6)	–482 ± 128 (6)	–162.9 ± 59.0 (6)	42.0 ± 19.0 (6)
90% max. current rise time (ms)	22.0 ± 0.4 (6)	541 ± 85 (6)	2.6 ± 0.2 (6)	ND	727 ± 36 (5)

$P < 0.05$ for all treatments *versus* control. Number of experiments are indicated between brackets.
HEK-KWGF, human embryonic kidney cell line stably expressing GFP-tagged inward rectifier channel protein $K_{IR}2.1$; ND, not determined.

The mutations E224A, D259A and E299A all significantly diminish this outward current block to about 50%, whereas the F254A mutation did not affect outward block, in contrast to its effect on chloroquine-mediated block (Rodríguez-Menchaca *et al.*, 2008).

In the heart, I_{K1} ion channels are formed by either homo- or heterotetramers of $K_{IR}2.1$, $K_{IR}2.2$ and $K_{IR}2.3$. We therefore assessed the effect of acute pentamidine block on homotetramers of murine $K_{IR}2.2$ and $K_{IR}2.3$ using the inside-out voltage clamp configuration. Figure 4C and D shows that pentamidine sensitivity was significantly reduced in homomers of $K_{IR}2.3$ compared with that observed for homomers of $K_{IR}2.1$. $K_{IR}2.2$ sensitivity for pentamidine block is in between that of $K_{IR}2.1$ and $K_{IR}2.3$ channels. Amino-acid alignment of the cytoplasmic pore region from $K_{IR}2.1$, 2.2 and 2.3 reveals complete identity for E224, D259 and E299 (Figure 4E). Overall, we conclude that cardiac I_{K1}, irrespective of its underlying molecular determinants, was susceptible to pentamidine-mediated acute block.

Inward rectification of I_{K1} ion channels is accomplished by the binding of endogenous polyamines inside the cytoplasmic and transmembrane regions of the pore (Lu, 2004). The negatively charged amino acids E224, D259 and E299 in the cytoplasmic region of the pore are likely to be involved in the polyamine-induced rectification (Fujiwara and Kubo, 2006; Tai *et al.*, 2009). To assess whether pentamidine block is affected by the presence of polyamines, pentamidine was applied in the presence of spermine. With low concentrations of spermine (0.1 μM), the outward component of I_{K1} displayed in a bi-phasic block (Figure 5A and B), presumably due to interactions of spermine with the transmembrane region (peak 1) and with the cytoplasmic region (peak 2) (Ishihara and Ehara, 2004; Ishihara and Yan, 2007). Co-application of pentamidine largely inhibited the cytoplasmic spermine binding region (peak 2), leaving the transmembrane region relatively unaffected (Figure 5). These results indicate that pentamidine enters and blocks the I_{K1} channel pore, but most likely does not penetrate as far as spermine. Thus, pentamidine-mediated I_{K1} block is not dependent on the presence of the polyamine spermine.

Discussion and conclusions

$K_{IR}2.x$ ion channel blockers

Very few drugs that block acutely the $K_{IR}2.1$ ion channels have had their mode of action resolved so far. Block mediated by tamoxifen, 4-hydroxy-tamoxifen and raloxifene is voltage independent and has been suggested to act by interfering with the $K_{IR}2.1$-PIP_2 interaction, outside the pore region (Ponce-Balbuena *et al.*, 2009). Chloroquine was found to inhibit the $K_{IR}2.1$ based I_{K1} channel in a voltage dependent mode by plugging the cytoplasmic pore region (Rodríguez-Menchaca *et al.*, 2008). We observed voltage-dependent pentamidine block, that is the outward component of I_{K1} was more strongly affected than the inward component, and altered kinetics with respect to maximum current rise time upon hyperpolarization. In addition, our molecular docking simulations identified a binding site for pentamidine in the cytoplasmic pore domain of $K_{IR}2.1$. The binding site is flanked by negatively charged residues E224, D259 and E229, which is in agreement with our alanine substitution results. Therefore, our data suggest that pentamidine acts by plugging the conduction pore, as has already been suggested for chloroquine (Rodríguez-Menchaca *et al.*, 2008). Both drugs seem to interact with $K_{IR}2.1$ primarily by electrostatic interactions. Our modelling on the closed state $K_{IR}2.1$ model did not provide evidence for drug interaction in the transmembrane cavity. Due to the lack of a working open state model, we cannot rule out the possibility of direct interaction of pentamidine with the transmembrane cavity for an open channel, which would result in drug-channel interaction at additional amino acid residues. The somewhat different behaviour of the inward component compared with the outward component in the different mutants with respect to pentamidine block would be compatible with this suggestion.

Of the above-mentioned drugs, only pentamidine displays specificity towards I_{K1}, while chloroquine, tamoxifen and raloxifene block additional cardiac ion channels (Liu *et al.*, 1998; He *et al.*, 2003; Liew *et al.*, 2004; Liu *et al.*, 2007; White, 2007). However, pentamidine is known to affect cardiac I_{Kr} in a 'non-acute' mode by interfering in forward trafficking of hERG mediated channels (Cordes *et al.*, 2005; Kuryshev *et al.*, 2005). With respect to $K_{IR}2.1$, we observed a decrease in protein expression levels over a relatively long timescale, and after the time at which direct channel block was evident. Expression level decreased faster in HEK-KWGF cells compared with adult cardiomyocytes, which may be explained by differences in $K_{IR}2.1$ half-life in the ectopic expression system compared with native $K_{IR}2.1$-expressing cells. However, a difference in pentamidine uptake, which is transporter dependent (Ming *et al.*, 2009), could also account for the observed temporal differences.

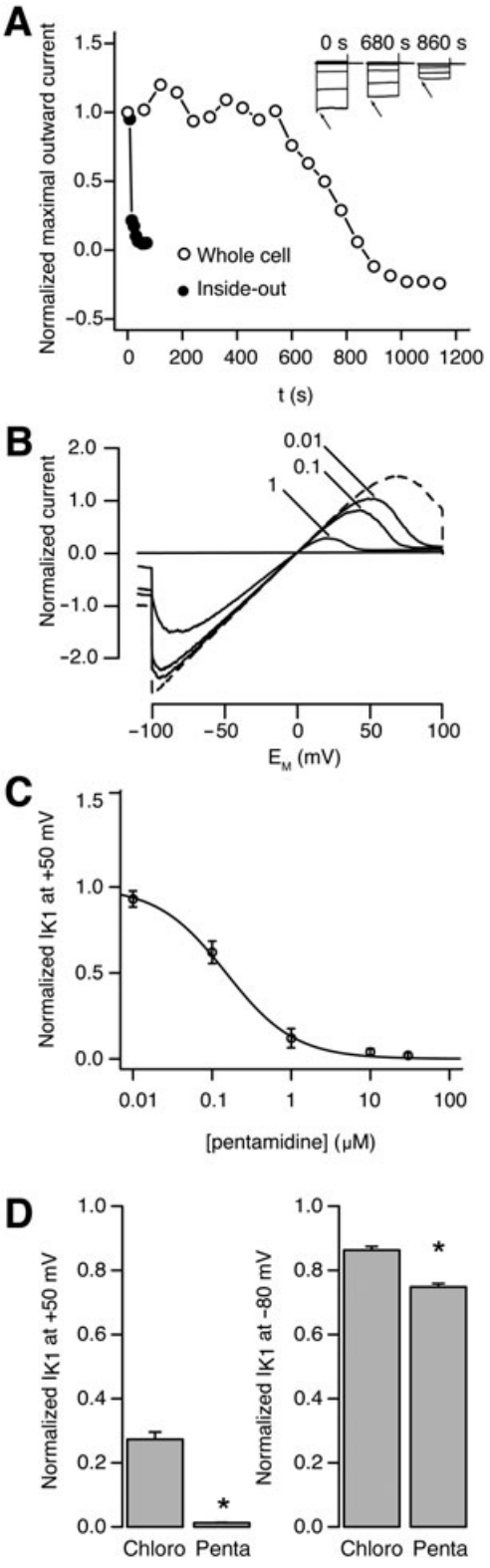

Figure 2 Pentamidine dose-response relationship for $K_{IR}2.1$ mediated I_{K1}. Typical recordings demonstrating a much slower developing pentamidine (10 μM)-induced I_{K1} block in whole cells, compared with inside-out recordings. Inset: Current traces during drug application in the whole cell configuration display altered channel kinetics (arrows). Control cells displayed no rundown for at least 20 min (A). Typical inside-out recording depicting inhibition of I_{K1} with increasing concentrations of pentamidine, demonstrating strongest effects on outward current. Dashed trace is the control recording (B). Average concentration-response curve for I_{K1} recorded in the inside-out configuration (n = 11) (C). Comparison of the inhibitory effect of chloroquine and pentamidine (both 1 μM) measured in inside-out experiments. Pentamidine has a significantly stronger blocking effect at this concentration, particularly for outward currents (D).

Clinical use and pharmacology of pentamidine

The second-line drug pentamidine is widely used and advocated in treatment of diverse forms of leishmaniasis (WHO estimation of 12 million infections worldwide, 1.5–2 million new cases each year) and human African trypanosomiasis (WHO estimation 70 thousand infections) (Lai A Fat *et al.*, 2002; Werbovetz, 2006). In the Western world, it has been used for the treatment of *P. carinii* pneumonia in HIV-positive patients, but its use is decreasing due to improved control of the primary infection in this patient group. Nevertheless, pentamidine use may increase due to the import (Zeegelaar *et al.*, 2005) and the northward spread (Dujardin *et al.*, 2008) of leishmaniasis in the Western world and in developing countries, as leishmaniasis becomes resistant to first-line medication (Croft *et al.*, 2006). Intravenous application of clinical doses (4 mg·kg^{-1}) results in plasma levels of 1.5–5 μM (Sands *et al.*, 1985; Goa and Campoli-Richards, 1987; Lidman *et al.*, 1994), comparable with the concentrations used in our *in vitro* experiments and in studies on $K_v11.1$ (hERG) (Cordes *et al.*, 2005; Kuryshev *et al.*, 2005). Although pentamidine directly interacts with the I_{K1} channel, block in the whole cell configuration occurs only after a short lag-time of 10 min, suggesting a relatively slow entrance of pentamidine into the cell. Indeed, pentamidine uptake in mammalian cells was defined recently as an organic cation transporter dependent process (Ming *et al.*, 2009). In mice, rats and humans, pentamidine accumulates in tissues with a strong preference for liver and kidney, while brain tissue remains virtually devoid of the drug (Waalkes *et al.*, 1970; Waldman *et al.*, 1973; Donnelly *et al.*, 1988). Neurons, like cardiac myocytes, express high levels of functional $K_{IR}2.x$ ion channels. The absence of pentamidine in brain tissue may explain the absence of strong neurological disorders during pentamidine therapy.

Experimental use of pentamidine and future perspectives

In contrast to several other ion currents like I_{Kr} and I_{Ks}, the contribution of I_{K1} to repolarization redundancy, known as repolarization reserve (Roden, 1998), has not been studied extensively *in vivo*. This is mainly due to the limited availability of specific I_{K1} inhibitors applicable to large animal models. The specific I_{K1} inhibitor Ba^{2+} is of limited use in *in vivo* studies due to reported lethality mainly caused by respiratory arrest (Roza and Berman, 1971). The I_{K1} pore blockers chloroquine (Rodríguez-Menchaca *et al.*, 2008) and pentamidine may, in principle, serve as an alternative for Ba^{2+} in experimental use. The disadvantages of chloroquine are its effects on protein degradation (Jansen *et al.*, 2008) and direct block of other cardiac ion channels (White, 2007). Pentamidine, on the other hand, may be used as a direct I_{K1} blocker, but long-term

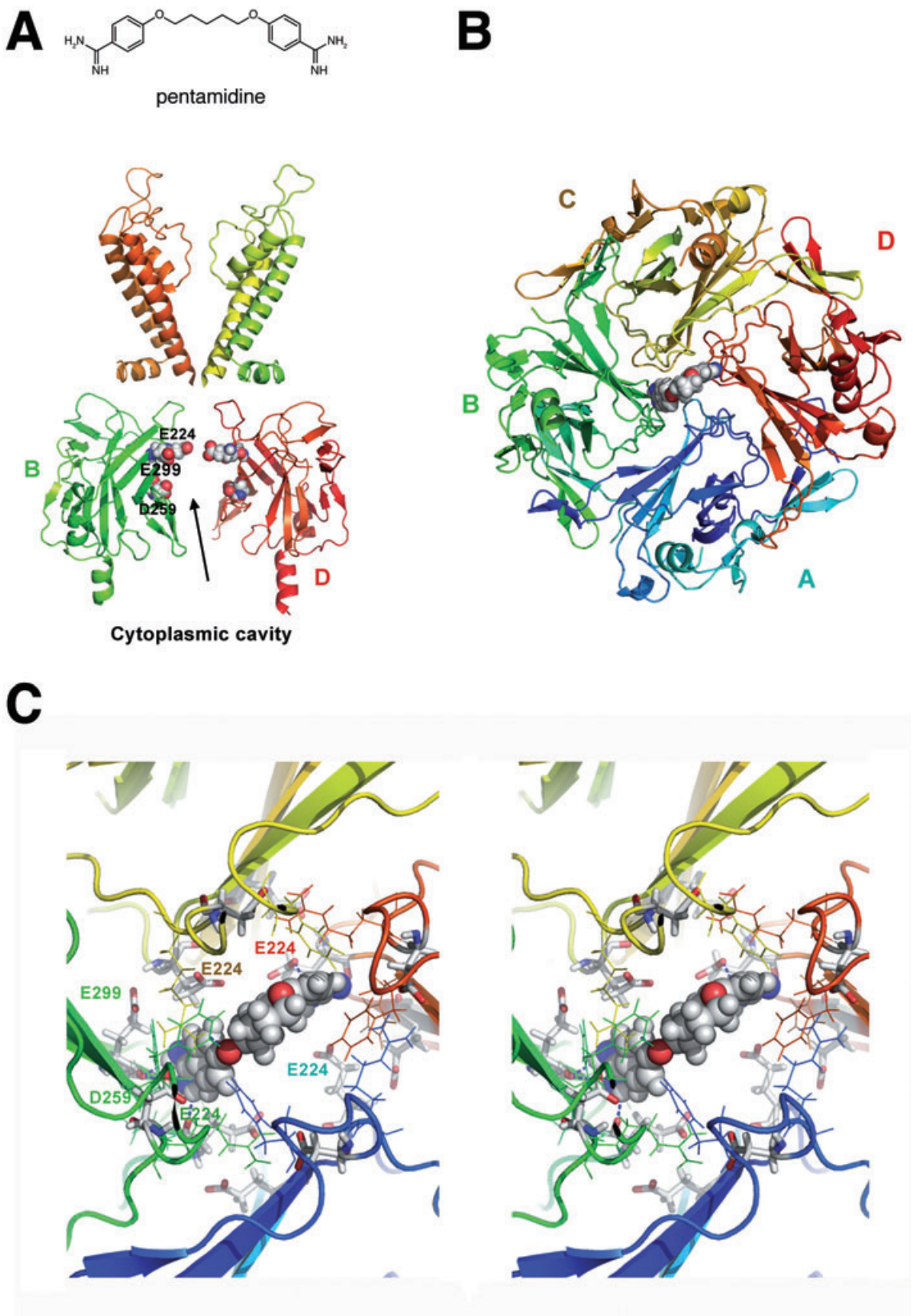

Figure 3 Docking of pentamidine within the $K_{IR}2.1$ cytoplasmic domain. Side view of 2 $K_{IR}2.1$ domains. The transmembrane regions (homology model of $K_{IR}2.1$, unpublished) and cytoplasmic domain (1U4F, crystal structure) with acidic residues E224, D259, E299 important for pentamidine block, highlighted (A). Bottom view of the preferential orientation of pentamidine in the cytoplasmic pore domain (B). Stereo view of the cytoplasmic pore domain with pentamidine plugging the pore. Residues are coloured according to domains (A = blue, B = green, C = orange, D = red) (C). All figures were prepared using the program PyMol (Delano Scientific).

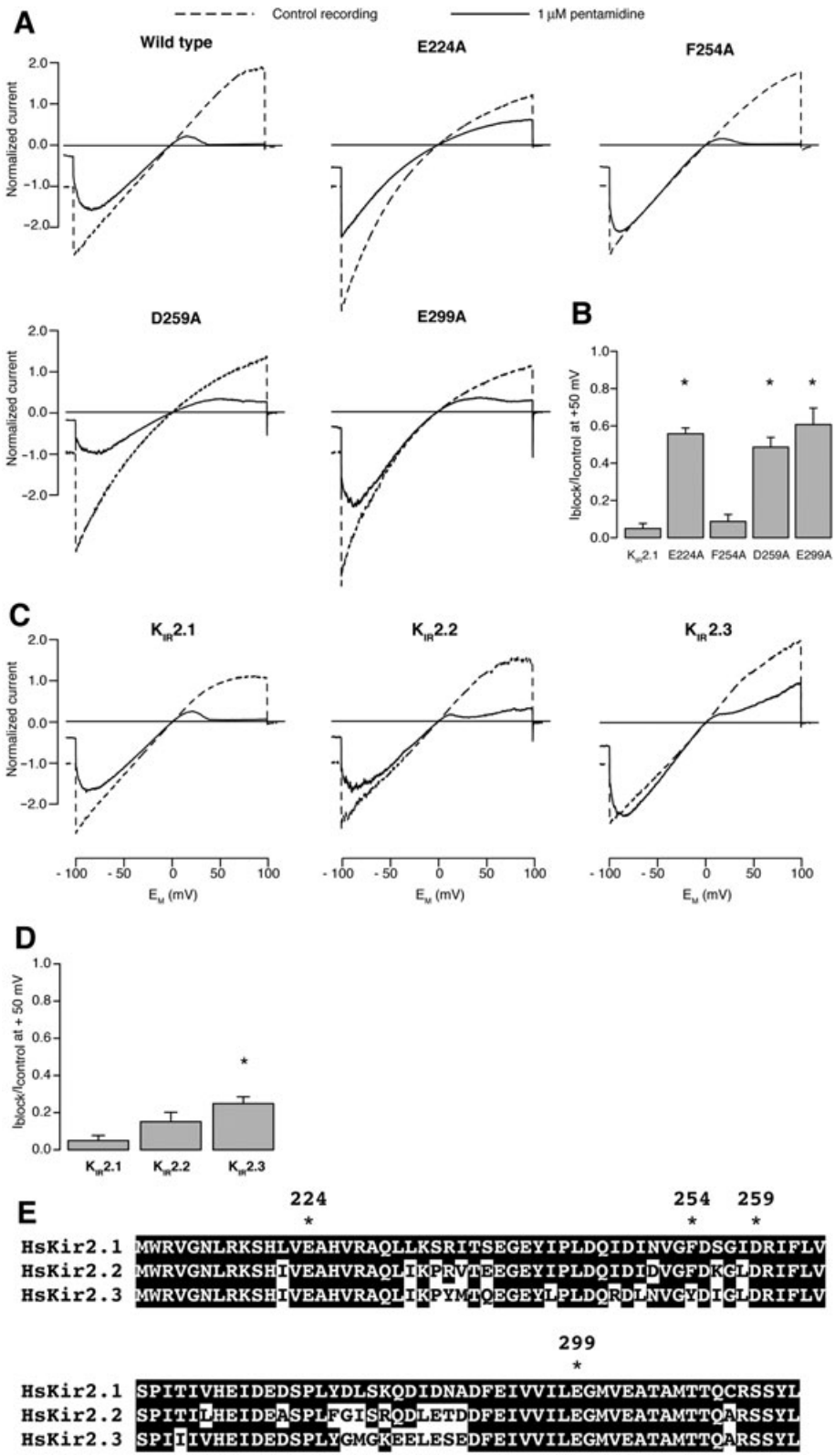

Figure 4 Pentamidine interacts with specific residues lining the $K_{IR}2.1$ channels pore region. Inside-out recordings of I_{K1} based on human $K_{IR}2.1$ in absence and presence of 1 μM pentamidine. In panel A, are recordings from alanine substitution mutants that demonstrate loss of normal pentamidine block of outward current when residues E224, D259 and E299 are substituted with alanine. In panel B, plot of average residual I_{K1} (at 50 mV) for the mutants depicted in panel A, normalized to control current levels. In panels C and D, inside-out recordings of I_{K1} based on mouse $K_{IR}2.1$, −2.2 and −2.3 in the absence and presence of 1 μM pentamidine, showing reduced pentamidine sensitivity of channels composed of $K_{IR}2.2$ and $K_{IR}2.3$ tetramers. In panel E, the amino acid alignment of the cytoplasmic pore region of human $K_{IR}2.1$, −2.2 and −2.3. Amino acid residues mutations tested for pentamidine block are indicated by asterisks. Murine sequences in this region are identical to the human forms (not shown). F254 is not conserved in $K_{IR}2.3$. Identical residues are indicated in white lettering and black shading.

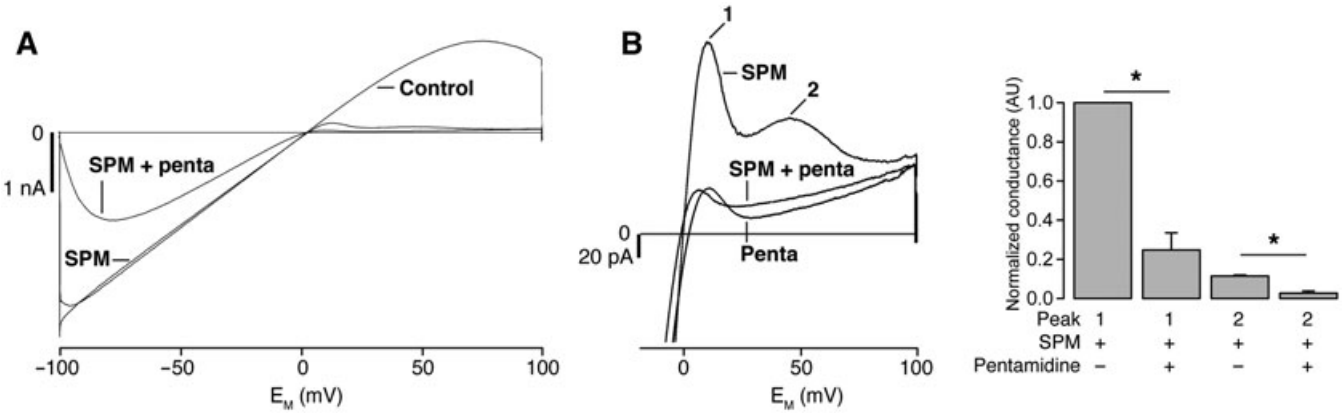

Figure 5 Pentamidine block is independent of spermine. Inside-out recording of mouse $K_{IR}2.1$ based I_{K1} in the absence of spermine and pentamidine (control), in the presence of 0.1 μM spermine (SPM) or with the combination of 1 μM pentamidine and spermine (SPM + penta) (A). Enlargement of panel A illustrates that outward I_{K1} block by 1 μM pentamidine is not different when pentamidine is added in the presence or absence of 0.1 μM spermine (averaged traces of 3, 3 and 4 patches, respectively) (B, left panel). The numbered peaks correspond with mode 1 and 2 block of I_{K1} channels by spermine (Ishihara and Ehara, 2004). Conductance of these peaks was significantly diminished by pentamidine; mode 2 block seems especially sensitive to pentamidine. Values were normalized using the mode 1 conductance recorded in presence of spermine for each recording (B, right panel).

application may lead to 'trafficking' defects of $K_v11.1$ and $K_{IR}2.1$ channel proteins also. Recently, pentamidine infusion in dogs was reported to induce mild QT(c) prolongation, which was suggested to be caused by unexpectedly rapid I_{Kr} channel trafficking defects (Yokoyama *et al.*, 2009). Based on our results described here, we would propose that the mild QT(c) prolongation in sinus rhythm (Yokoyama *et al.*, 2009) and chronic AV block (our unpublished observations) dogs is caused by acute I_{K1} block.

A potential clinical use for specific I_{K1} blockers can be found in gain-of-function mutations in the *KCNJ2* gene resulting in exacerbation of $K_{IR}2.1$-based I_{K1} associated with atrial fibrillation (Xia *et al.*, 2005; Zhang *et al.*, 2005b; Ehrlich, 2008). As elegantly shown by El Harchi *et al.* (2009), mutant channels are susceptible to chloroquine inhibition, presenting new opportunities for drug-based treatments.

Irrespective of the clinical utility of I_{K1} blocking drugs, target specificity is crucially required. Therefore, the molecular modelling studies on the interactions of chloroquine (Rodríguez-Menchaca *et al.*, 2008) and pentamidine (this study) with the $K_{IR}2.1$-based I_{K1} channel may promote further development of more specific I_{K1} channel blockers, applicable for both *in vivo* experimentation and therapeutic use.

Acknowledgements

We would like to thank Dr J. Miyazaki and Dr Y. Kurachi (Osaka University, Japan), Dr L. Jan (University of California San Francisco, USA) and Dr K. Ishihara (Saga University, Japan) for providing us with the pCXN2 and KCNJ2, –4 and –12 constructs; Dr Tristani-Firouzi (University of Utah School of Medicine, USA) for pore mutation constructs; This work was supported by a grant from Top Institute Pharma (D2-101), Leiden, the Netherlands (L.N., A.S.).

Conflict of interest

The authors state no conflict of interest.

References

Alexander SPH, Mathie A, Peters JA (2009). Guide to Receptors and Channels (GRAC), 4th edn. *Br J Pharmacol* **158** (Suppl. 1): S1–S254.

Bibler MR, Chou TC, Toltzis RJ, Wade PA (1988). Recurrent ventricular tachycardia due to pentamidine-induced cardiotoxicity. *Chest* **94**: 1303–1306.

Bray PG, Barrett MP, Ward SA, De Koning HP (2003). Pentamidine uptake and resistance in pathogenic protozoa: past, present and future. *Trends Parasitol* **19**: 232–239.

Cordes JS, Sun Z, Lloyd DB, Bradley JA, Opsahl AC, Tengowski MW *et al.* (2005). Pentamidine reduces hERG expression to prolong the QT interval. *Br J Pharmacol* **145**: 15–23.

Croft SL, Sundar S, Fairlamb AH (2006). Drug resistance in leishmaniasis. *Clin Microbiol Rev* **19**: 111–126.

De Boer TP, Van der Heyden MAG, Rook MB, Wilders R, Broekstra R, Kok B *et al.* (2006a). Pro-arrhythmogenic potential of immature cardiomyocytes is triggered by low coupling and cluster size. *Cardiovasc Res* **71**: 704–714.

De Boer TP, Van Veen TA, Houtman MJ, Jansen JA, Van Amersfoorth SC, Doevendans PA *et al.* (2006b). Inhibition of cardiomyocyte automaticity by electrotonic application of inward rectifier current from $K_{IR}2.1$ expressing cells. *Med Biol Eng Comput* **44**: 537–542.

Dhamoon AS, Jalife J (2005). The inward rectifier current (I_{K1}) controls cardiac excitability and is involved in arrhythmogenesis. *Heart Rhythm* **2**: 316–324.

Donnelly H, Bernard EM, Rothkotter H, Gold JWM, Armstrong D (1988). Distribution of pentamidine in patients with AIDS. *J Infect Dis* **157**: 985–989.

Dujardin JC, Campino L, Cañavate C, Dedet JP, Gradoni L, Soteriadou K *et al.* (2008). Spread of vector-borne diseases and neglect of leishmaniasis, Europe. *Emerg Infect Dis* **14**: 1013–1018.

Ehrlich JR (2008). Inward rectifier potassium currents as a target for atrial fibrillation therapy. *J Cardiovasc Pharmacol* **52**: 129–135.

Eisenhauer MD, Eliasson AH, Taylor AJ, Coyne PE Jr, Wortham DC (1994). Incidence of cardiac arrhythmias during intravenous pentamidine therapy in HIV-infected patients. *Chest* **105**: 389–394.

El Harchi A, McPate MJ, Zhang YH, Zhang H, Hancox JC (2009). Action potential clamp and chloroquine sensitivity of mutant $K_{IR}2.1$ channels responsible for variant 3 short QT syndrome. *J Mol Cell Cardiol* **47**: 743–747.

Fujiwara Y, Kubo Y (2006). Functional roles of charged amino acid

residues on the wall of the cytoplasmic pore of $K_{IR}2.1$. *J Gen Physiol* **127**: 401–419.

Girgis I, Gualberti J, Langan L, Malek S, Mustaciuolo V, Costantino T *et al*. (1997). A prospective study of the effect of I.V. pentamidine therapy on ventricular arrhythmias and QTc prolongation in HIV-infected patients. *Chest* **112**: 646–653.

Goa KL, Campoli-Richards DM (1987). Pentamidine isethionate: a review of its antiprotozoal activity, pharmacokinetic properties and therapeutic use in *Pneumocystis carinii* pneumonia. *Drugs* **33**: 242–258.

Gonzalez A, Sager PT, Akil B, Rahimtoola SH, Bhandari AK (1991). Pentamidine-induced torsade de pointes. *Am Heart J* **122**: 1489–1492.

He J, Kargacin ME, Kargacin GJ, Ward CA (2003). Tamoxifen inhibits Na^+ and K^+ currents in rat ventricular myocytes. *Am J Physiol Heart Circ Physiol* **285**: H661–H668.

Irwin JJ, Shoichet BK (2005). ZINC – a free database of commercially available compounds for virtual screening. *J Chem Inf Model* **45**: 177–182.

Ishihara K, Ehara T (2004). Two modes of polyamine block regulating the cardiac inward rectifier K^+ current I_{K1} as revealed by a study of the $K_{IR}2.1$ channel expressed in a human cell line. *J Physiol* **556**: 61–78.

Ishihara K, Yan DH (2007). Low-affinity spermine block mediating outward currents through $K_{IR}2.1$ and $K_{IR}2.2$ inward rectifier potassium channels. *J Physiol* **583**: 891–908.

Jansen JA, De Boer TP, Wolswinkel R, Van Veen TA, Vos MA, Van Rijen HV *et al*. (2008). Lysosome mediated $K_{IR}2.1$ breakdown directly influences inward rectifier current density. *Biochem Biophys Res Commun* **367**: 687–692.

Kannankeril PJ, Roden DM (2007). Drug-induced long QT and torsade de pointes: recent advances. *Curr Opin Cardiol* **22**: 39–43.

Kuryshev YA, Ficker E, Wang L, Hawryluk P, Dennis AT, Wible BA *et al*. (2005). Pentamidine-induced long QT syndrome and block of hERG trafficking. *J Pharmacol Exp Ther* **312**: 316–323.

Lai A Fat EJSK, Vrede MA, Soetosenojo RM, Lai A Fat RFM (2002). Pentamidine, the drug of choice for the treatment of cutaneous leishmaniasis in Surinam. *Int J Dermatol* **41**: 796–800.

Lidman C, Bronner U, Gustafsson LL, Rombo L (1994). Plasma pentamidine concentrations vary between individuals with *Pneumocystis carinii* pneumonia and the drug is actively secreted by the kidney. *J Antimicrob Chemother* **33**: 803–810.

Liew R, Stagg MA, MacLeod KT, Collins P (2004). Raloxifene acutely suppresses ventricular myocyte contractility through inhibition of the l-type calcium current. *Br J Pharmacol* **142**: 89–96.

Liu H, Jin MW, Xiang JZ, Huang Y, Sun HY, Chiu SW *et al*. (2007). Raloxifene inhibits transient outward and ultra-rapid delayed rectifier potassium currents in human atrial myocytes. *Eur J Pharmacol* **563**: 61–68.

Liu XK, Katchman A, Ebert SN, Woosley RL (1998). The antiestrogen tamoxifen blocks the delayed rectifier potassium current, I_{Kr}, in rabbit ventricular myocytes. *J Pharmacol Exp Ther* **287**: 877–883.

Lu Z (2004). Mechanism of rectification in inward-rectifier K^+ channels. *Annu Rev Physiol* **66**: 103–129.

Miake J, Marbán E, Nuss HB (2002). Biological pacemaker created by gene transfer. *Nature* **419**: 132–133.

Ming X, Ju W, Wu H, Tidwell RR, Hall JE, Thakker DR (2009). Transport of dicationic drugs pentamidine and furamidine by human organic cation transporters. *Drug Metab Dispos* **37**: 424–430.

Mitchell P, Dodek P, Lawson L, Kiess M, Russell J (1989). Torsades de pointes during intravenous pentamidine isethionate therapy. *Can Med Assoc J* **140**: 173–174.

Murphy CA, Dargie HJ (2007). Drug-induced cardiovascular disorders. *Drug Saf* **30**: 783–804.

Nagase S, Fukushima Kusano K, Yoshida M, Ohe T (2007). Electrophysiologic characteristics of an Andersen syndrome patient with *KCNJ2* mutation. *Heart Rhythm* **4**: 512–515.

Pegan S, Arrabit C, Zhou W, Kwiatkowski W, Collins A, Slesinger PA *et al*. (2005). Cytoplasmic domain structures of $K_{IR}2.1$ and $K_{IR}3.1$ show sites for modulating gating and rectification. *Nat Neurosci* **8**: 279–287.

Plaster NM, Tawil R, Tristani-Firouzi M, Canún S, Bendahhou S, Tsunoda A *et al*. (2001). Mutations in $K_{IR}2.1$ cause the developmental and episodic electrical phenotypes of Andersen's syndrome. *Cell* **105**: 511–519.

Ponce-Balbuena D, López-Izquierdo A, Ferrer T, Rodríguez-Menchaca AA, Aréchiga-Figueroa IA, Sánchez-Chapula JA (2009). Tamoxifen inhibits $K_{IR}2.x$ family of inward rectifier channels by interfering with PIP_2-channel interactions. *J Pharmacol Exp Ther* **331**: 563–573.

Quadrel MA, Atkin SH, Jaker MA (1992). Delayed cardiotoxicity during treatment with intravenous pentamidine: two case reports and a review of the literature. *Am Heart J* **123**: 1377–1379.

Roden DM (1998). Taking the 'idio' out of 'idiosyncratic': predicting Torsades des Pointes. *Pacing Clin Electrophysiol* **21**: 1029–1034.

Rodríguez-Menchaca AA, Navarro-Polanco RA, Ferrer-Villada T, Rupp J, Sachse FB, Tristani-Firouzi M *et al*. (2008). The molecular basis of chloroquine block of the inward rectifier $K_{IR}2.1$ channel. *Proc Natl Acad Sci USA* **105**: 1364–1368.

Roza O, Berman LB (1971). The pathophysiology of barium: hypokalemic and cardiovascular effects. *J Pharmacol Exp Ther* **177**: 433–439.

Sands M, Kron MA, Brown RB (1985). Pentamidine: a review. *Rev Infect Dis* **7**: 625–633.

Tai K, Stansfeld J, Sansom MSP (2009). Ion-blocking sites of the $K_{IR}2.1$ channel revealed by multiscale modeling. *Biochemistry* **48**: 8758–8763.

Tristani-Firouzi M, Jensen JL, Donaldson MR, Sansone V, Meola G, Hahn A *et al*. (2002). Functional and clinical characterization of *KCNJ2* mutations associated with LQT7 (Andersen syndrome). *J Clin Invest* **110**: 381–388.

Waalkes TP, Denham BA, DeVita VT (1970). Pentamidine: clinical pharmacologic correlations in man and mice. *Clin Pharmacol* **11**: 505–512.

Waldman RH, Pearce DE, Martin RA (1973). Pentamidine isothionate levels in lungs, livers, and kidneys of rats after aerosol or intramuscular administration. *Am Rev Respir Dis* **108**: 1004–1006.

Werbovetz K (2006). Diamidines as antitrypanosomal, antileishmanial and antimalarial agents. *Curr Opin Investig Drugs* **7**: 147–157.

White NJ (2007). Cardiotoxicity of antimalarial drugs. *Lancet Infect Dis* **7**: 549–558.

Xia M, Jin Q, Bendahhou S, He Y, Larroque MM, Chen Y *et al*. (2005). A $K_{IR}2.1$ gain-of-function mutation underlies familial atrial fibrillation. *Biochem Biophys Res Commun* **332**: 1012–1019.

Yokoyama H, Nakamura Y, Iwasaki H, Hoshiai K, Mitsumori Y, Sugiyama A (2009). Effects of acute intravenous administration of pentamidine, a typical hERG-trafficking inhibitor, on the cardiac repolarization process of halothane-anesthetized dogs. *J Pharmacol Sci* **110**: 476–482.

Zeegelaar JE, Steketee WH, Van Thiel PPAM, Wetsteyn JCFM, Kager FA, Faber WR (2005). Changing pattern of imported cutaneous leishmaniasis in the Netherlands. *Clin Exp Dermatol* **30**: 1–5.

Zhang L, Benson DW, Tristani-Firouzi M, Ptácek LJ, Tawil R, Schwartz PJ *et al.* (2005a). Electrocardiographic features in Andersen-Tawil syndrome patients with *KCNJ2* mutation. Characteristic T-U-wave patterns predict the *KCNJ2* genotype. *Circulation* **111**: 2720–2726.

Zhang H, Garratt CJ, Zhu J, Holden AV (2005b). Role of up-regulation of I_{K1} in action potential shortening associated with atrial fibrillation in humans. *Cardiovasc Res* **66**: 493–502.